0013-7227/08/$15.00/0
*Printed in U.S.A.*

Endocrinology 149(7):3531–3539

doi: 10.1210/en.2007-1340

# Adrenal Hypersensitivity Precedes Chronic Hypercorticism in Streptozotocin-Induced Diabetes Mice

Yanina Revsin, Diane van Wijk, Flavia E. Saravia, Melly S. Oitzl, Alejandro F. De Nicola, and E. Ronald de Kloet

*Division of Medical Pharmacology (Y.R., D.v.W., M.S.O., E.R.d.K.), Leiden/Amsterdam Center for Drug Research (LACDR), Leiden University Medical Center, 2333CC Leiden, The Netherlands; and Laboratory of Neuroendocrine Biochemistry (Y.R., F.E.S., A.F.D.N.), Instituto de Biología y Medicina Experimental (IBYME), 1426 Buenos Aires, Argentina*

**Previous studies have demonstrated that type 1 diabetes is characterized by hypercorticism and lack of periodicity in adrenal hormone secretion. In the present study, we tested the hypothesis that hypercorticism is initiated by an enhanced release of ACTH leading subsequently to adrenocortical growth and increased output of adrenocortical hormones. To test this hypothesis, we used the streptozotocin (STZ)-induced diabetes mouse model and measured hypothalamic-pituitary-adrenal axis activity at different time points. The results showed that the expected rise in blood glucose levels induced by STZ treatment preceded the surge in corticosterone secretion, which took place 1 d after diabetes onset. Surprisingly, circulating ACTH levels were not increased and even below control levels until 1 d after diabetes onset and remained low until d 11 during hypercorticism. In response to ACTH (but not vasopressin), cultures of adrenal gland cells from 11-d diabetic mice secreted higher amounts of corticosterone than control cells. Real-time quantitative PCR revealed increased expression of melanocortin 2 and melanocortin 5 receptors in the adrenal glands at 2 and 11 d of STZ-induced diabetes. AVP mRNA expression in the paraventricular nucleus of the hypothalamus was increased, whereas hippocampal MR mRNA was decreased in 11-d diabetic animals. GR and CRH mRNAs remained unchanged in hippocampus and paraventricular nucleus of diabetic mice at all time points studied. These results suggest that sensitization of the adrenal glands to ACTH rather than an increase in circulating ACTH level is the primary event leading to hypercorticism in the STZ-induced diabetes mouse model. (*Endocrinology* 149: 3531–3539, 2008)**

TYPE 1 DIABETES (T1D) is a common metabolic disorder characterized by profound dysregulation of the hypothalamic-pituitary-adrenal (HPA) axis and disturbances in central nervous system functions (1–7). Among the alterations in the central nervous system functions, we previously reported enhanced expression of markers for astrogliosis and oxidative stress in the hippocampus of uncontrolled streptozotocin (STZ)-induced diabetic mice (8, 9). The hippocampus plays a crucial role in processes underlying learning and memory (10, 11) and has a transsynaptic neural input to CRH neurons in the paraventricular nucleus of the hypothalamus (PVN) (12). This hippocampal output to the PVN is known to inhibit HPA axis activity under basal and stressful conditions (13). Thus, it is conceivable that alterations in hippocampal markers could reflect disturbance in hippocampal output, which in turn could contribute to HPA axis dysregulation, leading to hypercorticism in the diabetic animals (14).

Previous reports indeed have shown alterations at various levels of the HPA axis such as increased hippocampal mineralocorticoid receptor (MR) and hypothalamic CRH mRNA and circulating ACTH levels (15). These alterations are believed to underlie corticosterone (B) hypersecretion in diabetes (16). At the time of full-blown diabetes, increase in central drive to the HPA axis at and/or above the level of the PVN has been reported (15, 16). This increased HPA axis drive would operate in the face of decreased B negative feedback sensitivity when diabetes is developed at d 8 after STZ treatment. However, the initial trigger of the sustained activation of the HPA axis is not known.

The current study was designed to assess some of the initial changes in the HPA axis at the onset of diabetes (author's operational definition of the first measured hyperglycemia after STZ injection) that eventually lead to chronic B hypersecretion in T1D. Based on previous studies, the hypothesis was tested that hypercorticism would start with enhanced release of ACTH leading subsequently to adrenocortical growth and stimulation of its adrenal melanocortin receptors 2 and 5 (MC2 and MC5). To test this hypothesis, we measured various key components of HPA axis activity at different time points after administration of STZ into c57BL/6 mice. These include plasma ACTH and B levels as well as CRH and vasopressin (AVP) mRNAs expression in the PVN. MR and glucocorticoid receptor (GR) expression were measured in the hippocampus and PVN. Moreover, the expression of AVP 1a receptor (V1aR), MC2 receptor (MC2R), and MC5R were measured in the adrenals, whereas their ability to secrete B was tested with ACTH and AVP stimulation using adrenal cell culture.

We find that the initial hypersecretion of B at the onset of

**First Published Online April 17, 2008**

Abbreviations: AVP, Vasopressin; B, corticosterone; GR, glucocorticoid receptor; HPA, hypothalamic-pituitary-adrenal; MC2 and MC5, melanocortin receptors 2 and 5; MC2R, MC2 receptor; MR, mineralocorticoid receptor; NOD, nonobese diabetic; PVN, paraventricular nucleus of the hypothalamus; RNase, ribonuclease; RT-qPCR, real-time quantitative PCR; SSC, standard saline citrate; STZ, streptozotocin; T1D, type 1 diabetes; V1aR, AVP 1a receptor.

***Endocrinology* is published monthly by The Endocrine Society (http://www.endo-society.org), the foremost professional society serving the endocrine community.**

diabetes occurs as a result of adrenal gland hypersensitization to ACTH rather than being triggered by elevated ACTH levels.

## Materials and Methods

### Animals

Twelve-week-old c57BL/6 male mice (Janvier, Le Genest Saint Isle, France) were group housed (two or three mice per cage, randomly mixing vehicle- or STZ-injected animals) under constant humidity (55 ± 5%) and temperature (23 ± 2 C) conditions, with 12-h light, 12-h dark cycle (lights on at 0800 h) at the animal facility of the LACDR, Leiden. Food and water was provided *ad libitum*. The animal experiments were performed in accordance with the European Communities Council Directive 86/609/EEC and with approval from the animal care committee of the Faculty of Medicine, Leiden University (UDEC No. 04096).

### Treatment

Mice received a single ip dose of 170 mg/kg STZ (Sigma Chemical Co., St. Louis, MO) at 0900 h in 0.5 M sodium citrate buffer (pH 4.5) or vehicle; 48 h after injection, diabetes was assessed by glucose levels in blood in the nonfasting condition (Accu-Chek Compact; Roche Diagnostics, Mannheim, Germany). Plasma glucose level measurements and killing of mice were performed between 1000 and 1200 h for all the experiments, except for the time course studies of Fig. 2. Animals with glucose levels higher than 11 mM were classified as overtly diabetic.

### Experiments

Two and 11 d after diabetes onset (acute and chronic diabetes, respectively), animals were decapitated; brain and adrenal glands were quickly removed, frozen in isopentane, and stored at −80 C until processing for later use in *in situ* hybridization and real-time quantitative PCR (RT-qPCR) procedures, respectively. For adrenal cell cultures, adrenal glands were immediately processed for direct use, and trunk blood was collected for RIA measurements.

### In situ hybridization

Determination of mRNA levels of MR, GR, AVP, and CRH were measured on coronal brain cryosections (14 μm) containing hippocampus (distance from bregma, −1.7 to −2.06 mm) and PVN (distance from bregma, −0.7 to −1.06 mm) (17). Two or three sections from each mouse were mounted on slides coated with poly-L-lysine (Sigma) and stored at −80 C. The sections were fixed for 30 min in freshly made 4% paraformaldehyde (Sigma) in PBS (pH 7.4), rinsed twice in PBS, acetylated in triethanolamine (0.1 M, pH 8.0) with 0.25% acetic anhydride for 10 min, rinsed for 10 min in 2× standard saline citrate (SSC: 150 mM sodium chloride, 15 mM sodium citrate), dehydrated in an ethanol series, air dried, and stored at room temperature until the *in situ* hybridization. The cRNA probes for GR and MR (mouse, exon 2 coding region) (18, 19), CRH (rat, full-length coding region) (20), and AVP (rat, exon C coding region) (21) were used. The antisense cRNA probes were transcribed from a linearized plasmid. *In situ* hybridization was performed using labeled ribonucleotide probes (labeling reaction: 10% 10× transcription buffer, 20% nucleotide mix (33.3% 10 nM ATP plus 33.3% 10 nM CTP plus 33.3% 10 nM GTP), 12% 100 μM UTP, 4% ribonuclease (RNase) inhibitor, 5% riboprobe, 19% $ddH_2O$, 25% [$^{35}$S]UTP, 5% polymerase), reaching 80–90% transcription efficiency. A 100-μl aliquot of hybridization mix [50% formamide, 20% dextran sulfate, 1.2 mM EDTA (pH 8.0), 25 mM sodium phosphate (pH 7.0), 350 mM sodium chloride, 100 mM dithiothreitol and 1% Denhardt's, 2% RNA-DNA mix (50% t-RNA plus 50% herring sperm DNA), 0.2% nathiosulfate and 0.2% sodium dodecyl sulfate] containing $2 \times 10^6$ dpm from each riboprobe was added to each slide. Coverslips were put on the slides, which were hybridized overnight in a moist chamber at 55 C. The next morning, coverslips were removed and the sections washed in graded salt solutions at optimized temperature [10 min 2% SSC at 55 C, 15 min RNase A solution (0.2% RNase A plus 10% 5 M NaCl plus 1% 1 M Tris-HCl plus 88.8% $dH_2O$) at 37 C, two times for 10 min each 2% SSC at 65 C, 15 min 2% SSC/formamide at 65 C, 10 min 1% SSC at 65 C, and 10 min 0.1% SSC at 65 C]. After the washing steps, sections were dehydrated in a series of ethanol baths and air dried. The signal was quantified from film Kodak Biomax MR film (Eastman Kodak Co., Rochester, NY) and developed. Autoradiographs were digitized, and relative expression of MR, GR, CRH, and AVP mRNA was determined by computer-assisted optical densitometry (analysis 3.1; Soft Imaging System GmbH). The mean of four to six measurements of each riboprobe was calculated for each animal.

### RIA

Trunk blood was collected individually in fasting (1700 and 2000 h) and nonfasting (0900 and 1300 h) conditions in labeled potassium-EDTA-coated tubes (1.6 mg EDTA/ml blood; Sarstedt AG & Co., Nümbrecht, Germany). Blood samples were kept on ice and later centrifuged for 15 min at 3000 rpm at 4 C. Plasma was transferred to clean tubes and stored frozen at −20 C until the determination of ACTH and B by the MP Biomedical RIA kit (ICN Biomedicals Inc., Costa Mesa, CA). Insulin concentrations were measured with a RIA kit following the manufacturer's instructions (Linco Research, St. Charles, MO).

### RT-qPCR

Total RNA was extracted from the adrenals using TRIzol RNA isolation reagent (Invitrogen) according to the manufacturer's recommendations.

After isolation, total RNA was purified using the QIAGEN RNEasy Mini Kit RNA Cleanup (QIAGEN Inc., Valencia, CA) according to the manufacturer's instructions. RNA quality was assessed with the Nanodrop (Isogen Life Science, Maarsen, The Netherlands).

Before cDNA synthesis, all RNA samples were treated with deoxyribonuclease I (Invitrogen Life Technologies), according to the manufacturer's protocol. Synthesis of cDNA was performed in a total volume of 20 μl, using SuperScript II reverse transcriptase (Invitrogen Life Technologies). Each experimental sample of RNA (10 ng/μl) was placed into the cDNA-synthesis reaction. Standard curves were generated by performing cDNA-synthesis reactions on 100, 50, 25, 12.5, 6.25, 3.125, 1.562, and 0.78 ng/μl input RNA. As a control for genomic contamination, $RT^-$ samples were used.

Primers for ACTH receptors, MC2R (forward 5′-AAATGATTCTGCTGCTTCCAA-3′ and reverse 5′-TGGTGTTTGCCGTTGACTTA-3′), MC5R (forward 5′-TGGAACCCGTGAAGAATCAT-3′ and reverse 5′-TCCTAAAATGCCATCCTCTGA-3′), and V1aR (forward 5′-GCCTACATCCTCTGCTGGAC-3′ and reverse 5′-AGCTGTTCAAGGAAGCCAGT-3′) were designed using the Ensemble database, Primer3, and the NCBI database BLAST, all accessible on the internet. The amount of the target genes was determined relative to the housekeeping gene 18S (forward 5′-GTAACCCGTTGAACCCCATT-3′ and reverse 5′-CCATCCAATCGGTAGTAGCG-3′) (22).

Specificity of the primer sets was assessed with a cDNA sample (12.5 ng/μl) and a negative, $RT^-$, sample using the LightCycler and LightCycler FastStart DNA Master$^{PLUS}$ SYBR Green I kit (Roche Diagnostics GmbH, Mannheim, Germany). Dissociation curves were examined for each primer pair and controlled for specificity of the reaction and genomic contamination by checking the $RT^-$ and no-template control samples. Then, for each primer pair, the standard curve (50, 25, 12.5, 6.25, 3.125, 1.562, and 0.78 ng/μl) was plotted, and the PCR efficiency was estimated. All used primer pairs displayed reaction efficiencies between 80 and 100%. Target gene cycle threshold values ranged from 18–32, whereas $RT^-$ and no-template control samples showed no products after 40 cycles.

PCR amplification of the cDNA was performed in a 20-μl reaction, using the LightCycler and LightCycler FastStart DNA Master$^{PLUS}$ SYBR Green I kit. A PCR MasterMix was made consisting of 7 μl PCR-graded water, 4 μl reaction mix, 4 μl PCR primers, and 5 μl cDNA. The LightCycler protocol started with a preincubation, heating for 10 min at 95 C, followed by 45 cycles of 10 sec at 95 C, 10 sec at 60 C, and 10 sec at 72 C for elongation. After the amplification, the program continued with a melting curve consisting of 15 sec at 65 C after which the temperature was held at 4 C.

### Adrenocortical cell culturing

Immediately after decapitation, the adrenals were removed, their fat was cleaned, their individual weight was determined, and they were stored in 0.9% NaCl. Cell suspension was made by cutting the tissue into small pieces and placing in 2 mg crude collagenase (Sigma-Aldrich Inc., Steinheim, Germany) and 0.4% BSA in 1 ml DMEM buffer (25 mM HEPES, 4500 mg/liter glucose; BioWhittaker, Cambrex BioScience, Verviers, Belgium). The cell suspension was disrupted continuously by pipetting every 15 min during the 2-h incubation at 37 C (atmosphere of 95% $O_2$ and 5% $CO_2$). The cell samples were then centrifuged twice at 100 × $g$ (4 C) for 10 min, and the cells were resuspended in 1.12 mg $CaCl_2$ in 1ml DMEM solution ($CaCl_2$ solution) and 0.4% BSA in DMEM. For testing the cell viability, cell suspensions were concentrated in the $CaCl_2$ solution and mixed with an equal volume of trypan blue (1 mg/ml in 0.9% NaCl), and cells containing liquid droplets and therefore excluding the dye (adrenocortical cells) were counted under the microscope. The volumes of the cell suspensions were adjusted to 10,000 adrenocortical cells/ml with 5% BSA in DMEM and distributed into Eppendorf tubes, each consisting of 0.9 ml cell suspension, to be incubated for 60 min at 37 C (at the described atmosphere).

The ACTH and AVP challenges were performed with $3.4 \times 10^{-9}$ M $ACTH_{1-24}$ (Synacthen; Novartis Pharma BV, Arnhem, The Netherlands), $10^{-6}$ M AVP ([Arg8] 1–8; Organon, Oss, The Netherlands) or 5% BSA in DMEM (nonchallenged is negative control of the experiment). After cell suspension incubation, 0.1 ml of each concentration was added, and the samples were incubated for 2 h at 37 C followed by centrifugation at 2500 × $g$ for 10 min (4 C). The supernatant was collected and stored at −20 C until later use for B determination by RIA.

### *Data analysis and statistics*

All data are expressed as mean ± SEM. Statistical analysis was performed using GraphPad Software (version 4). For pathophysiological measurements, six to seven mice per group were used and unpaired $t$ test was applied. For *in situ* hybridization, five to eight mice per group were used, the values were assessed by OD of the signal on autoradiographic film, and the statistical analysis was by nonparametric two-tailed Mann-Whitney $U$ test or two-way ANOVA plus Bonferroni post test. For RT-qPCR, five mice per group and two-way ANOVA plus Bonferroni post test was used. For adrenal cell cultures, six to seven mice per group were employed, and two-way ANOVA plus Bonferroni post test was applied. Statistical differences were considered significant when $P < 0.05$.

## Results

### *Pathophysiology*

The pathophysiology of the diabetic mice resembled the characteristic clinical features of the disease. Table 1 shows at d 2 and 11 after diabetes onset, increased glucose levels (>11 mM) and adrenal/body weight ratio, whereas body weight and thymus/body weight ratio were decreased. Absolute adrenal weights were similar at early time points after injection (4 h diabetic 1.77 ± 0.06, control 1.93 ± 0.04; 8 h diabetic 1.97 ± 0.06, control 2.06 ± 0.12; 24 h diabetic 1.87 ± 0.08, control 1.68 ± 0.06; 48 h diabetic 2.07 ± 0.09, control 2.0 ± 0.15 mg), and in 2-d diabetic mice and controls (diabetic 1.75 ± 0.10, controls 1.52 ± 0.07, mg). At 11 d after diabetes onset, adrenal weights were significantly higher (diabetic 2.83 ± 0.12, control 1.74 ± 0.16 mg, $P < 0.001$). Absolute thymus weight did not differ at the early time points after injection (4 h diabetic 23.18 ± 1.43, control 22.20 ± 1.51; 8 h diabetic 21.77 ± 2.0, control 20.62 ± 2.70; 24 h diabetic 17.95 ± 1.7, control 21.50 ± 1.30; 48 h diabetic 17.16 ± 1.37, control 23.72 ± 0.93 mg), however, it was significantly decreased in diabetic compared with control mice at d 2 (diabetic 6.39 ± 0.6, control 24.83 ± 1.97, $P < 0.0001$) and d 11 (diabetic 10.13 ± 1.29, control 29.32 ± 4.21 mg, $P < 0.01$) after diabetes onset. In addition, diabetic mice exhibited increased food and water intake from diabetes onset (data not shown).

### *Plasma glucose, insulin, B, and ACTH*

In diabetic mice, basal B levels increased significantly 1 d after diabetes onset, when circulating glucose levels rose above 11 mM (Fig. 1A) and were maintained at a high level until animals were killed. Control animals showed low basal B levels (<10 ng/ml) (Fig. 1B). Because diabetic mice have lost circadian rhythmicity in HPA axis activity, this accounts for variations in the basal B levels from different sets of animals observed at 48 h after STZ injection in Fig. 1, A and B. Although B levels were elevated, basal plasma ACTH in the same animals was significantly decreased after diabetes onset compared with controls (acute diabetic 69.97 ± 12.64, control 159.3 ± 27.54; chronic diabetic 70.94 ± 8.03, control 158.4 ± 20.31 ng/ml) (Fig. 1C). Surprisingly, the rise in B was not preceded by an increase in ACTH level in diabetic mice. A time course curve of ACTH at 4, 8, 24, 48, 59, 72, or 83 h after STZ injection (0900 h) showed no increase in ACTH at any time point compared with controls (Fig. 2A). At 4 h after injection, STZ-injected mice exhibited increased B concentration compared with vehicle-injected animals (Fig. 2B). However, in STZ-injected mice, B was comparable to control levels at 8, 24, 48, and 59 h after injection and commenced to increase from 72 h, *i.e.* at 1 d after diabetes onset (Fig. 2B).

To evaluate the metabolic implications after STZ injection, insulin concentrations were also measured in the same animals. Figure 2B shows the time course of insulin levels and reveals that circulating insulin levels significantly increase 8 h after STZ injection. This increase is followed by significant decrease from 48 h onwards (Fig. 2C).

**TABLE 1.** Pathophysiological measures of diabetic mice at 2 or 11 d after diabetes onset

| | Glycemia (mM) | Δ Body weight (g) | Adrenal/body weight ratio | Thymus/body weight ratio |
|---|---|---|---|---|
| 2 d after diabetes onset | | | | |
| Controls | 9.29 ± 0.53 | 3.33 ± 0.71 | 99.54 ± 4.43 | 1022 ± 91.84 |
| Diabetic | 25.90 ± 1.19[c] | 1.0 ± 0.52[a] | 158.9 ± 15.91[b] | 351.5 ± 35.33[c] |
| 11 d after diabetes onset | | | | |
| Controls | 9.643 ± 0.52 | 2.857 ± 0.51 | 66.95 ± 6.17 | 1129 ± 163.20 |
| Diabetic | 25.40 ± 2.07[c] | −3.833 ± 1.01[c] | 160.40 ± 10.94[c] | 580.50 ± 90.65[a] |

Glycemia, difference (Δ in grams) in body weight at the time of vehicle or STZ injections and at time of euthanasia, and adrenal/body weight and thymus/body weight ratios were assessed. Values are expressed as mean ± SEM; n = 6–7. Adrenal and thymus/body weight ratios are expressed as absolute weight × 1000 (g)/body weight (g).

[a] $P < 0.05$ *vs.* control.
[b] $P < 0.01$ *vs.* control.
[c] $P < 0.0001$ *vs.* control.

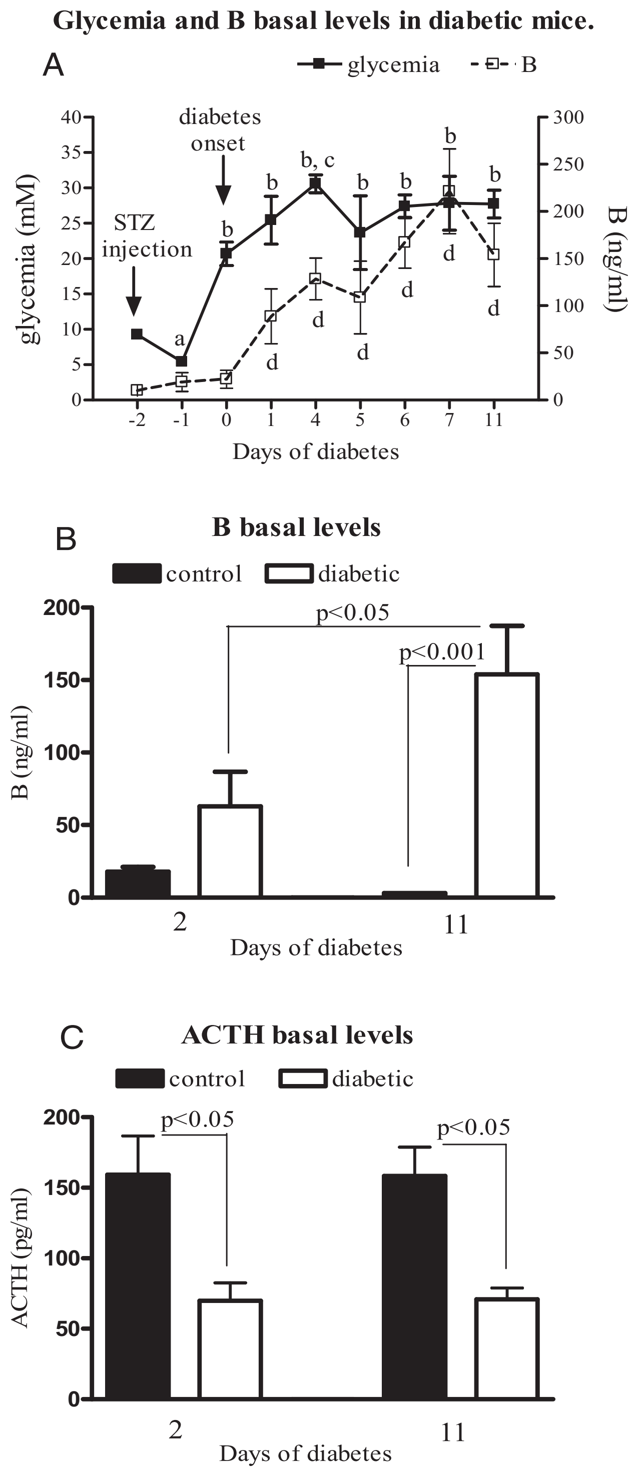


FIG. 1. Time course of blood glucose, basal plasma B, and ACTH levels. A, Changes in glucose and B levels after STZ injection; B and C, B (B) and ACTH (C) concentrations in control (*black bars*) and diabetic (*white bars*) mice at 2 and 11 d after STZ or vehicle injection. Blood samples were collected from tail snips between 0930 and 1030 h and are repeated measures from the same set of animals. Values are expressed as mean ± SEM; n = 6–8. For glycemia measurement: a, $P < 0.05$ *vs.* d −2; b, $P < 0.05$ *vs.* d −2 and −1; c, $P < 0.05$ *vs.* d 0. For B measurements: d, $P < 0.05$ *vs.* d −2, −1, and 0. Diabetes onset is according to the author's operational definition of the first measured hyperglycemia after STZ injection.

*Adrenal regulation*

*ACTH and AVP challenges in chronic diabetes.* Adrenocortical cells (10,000 cells per animal) were incubated with $3.4 \times 10^{-9}$ M $ACTH_{1–24}$, $10^{-6}$ M $AVP_{1–8}$, or 5% BSA in DMEM buffer as a negative control (nonchallenged). The ACTH concentration used for the challenge, which triggers B secretion in these cultures, was established by a dose-response curve to $1.7 \times 10^{-11}$, $3.4 \times 10^{-11}$, and $3.4 \times 10^{-9}$ M $ACTH_{1–24}$. In agreement with a previous report by Oitzl *et al.* (23), only the $3.4 \times 10^{-9}$ M dose triggers B release from control cell cultures, whereas the others do not have any effect. Figure 3A describes the response of the adrenal cells to $3.4 \times 10^{-9}$ M $ACTH_{1–24}$. Cultures of adrenal cells from diabetic mice secreted extremely high levels of B compared with cultures from control animals. Parallel cultures from the same mice challenged with $10^{-6}$ M $AVP_{1–8}$ showed different results. $AVP_{1–8}$ triggered B secretion in adrenal cell culture from control but not from diabetic animals (Fig. 3B).

*RT-qPCR ACTH receptor and V1aR mRNA.* The cDNA levels of the targeted genes were normalized with 18S cDNA expression. Adrenal ACTH receptor MC2 mRNA expression was significantly increased in acute and chronic STZ-diabetic mice ($P < 0.05$) (Fig. 4A), and MC5R mRNA was significantly increased in chronic diabetes ($P < 0.01$) (Fig. 4B). V1aR expression was not changed in diabetes (data not shown).

*HPA axis disturbances*

The *in situ* hybridization revealed no differences in hippocampal MR and GR mRNA expression between control and diabetic mice 2 d after the onset of the disease (Table 2). Chronic diabetic mice showed decreased MR mRNA in the hippocampus, which was significantly different only in the granular cells of the dentate gyrus (Table 2). The variation in mRNA expression between controls at 2 and 11 d (Table 2) represent the outcome of different experiments performed at different times in which the films were not adjusted against a standard. For that reason, the OD is expressed as arbitrary units from diabetic mice compared with control for each day. It is also noteworthy that significant MR mRNA up-regulation was found in the CA1 area of the hippocampus only on the day of diabetes onset (controls 20.43 ± 3.73, diabetics 34.80 ± 3.11 OD, arbitrary units; $P < 0.05$; n = 5).

In the PVN, the levels of AVP mRNA were significantly elevated in acute and chronic diabetic mice compared with controls (Table 2); CRH and GR mRNA expression did not differ between STZ-diabetic and vehicle-treated mice in acute and chronic diabetes (Table 2).

## Discussion

The present study shows that the rise in blood glucose levels induced by STZ treatment precedes the surge in B secretion in the STZ-induced diabetes mouse model. This increase in circulating B levels seems to be triggered by a rapidly enhanced sensitivity of the adrenals to ACTH. Hence, the sustained hypercorticism in the face of a dramatically enhanced adrenal sensitivity to ACTH seems already established very early in the onset of diabetes.

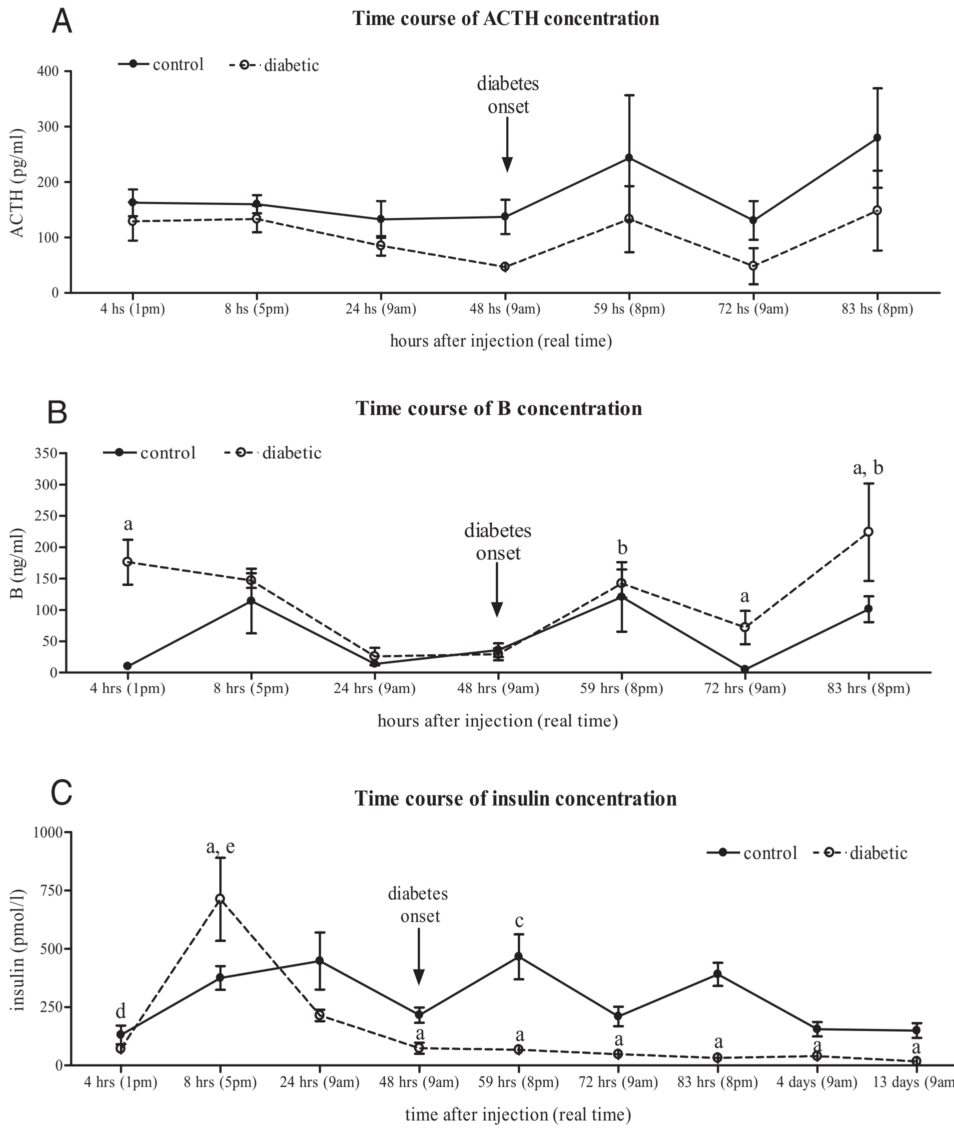


FIG. 2. Time course of plasma ACTH, B, and insulin concentrations. A, ACTH levels; B, B levels; C, insulin levels after 4 (1300 h), 8 (1700 h), 24 (0900 h), 48 (0900 h), 59 (2000 h), 72 (0900 h), and 83 (2000 h) hours after STZ or vehicle injection. Values expressed mean ± SEM; n = 4–6. a, $P < 0.05$ *vs.* control; b, $P < 0.05$ *vs.* diabetic at 48 h; c, $P < 0.05$ *vs.* 4, 48, and 72 h and 4 and 13 d; d, $P < 0.05$ *vs.* 83 h; e, $P < 0.05$ *vs.* 4, 24, 48, 59, 72, and 83 h and 4 and 13 d. Four and 13 d after STZ injection is the same as 2 and 11 d of diabetes, respectively. Diabetes onset is according to author's operational definition of the first measured hyperglycemia after streptozotocin injection.

Therefore, the current data reject the hypothesis that hypercorticism would start with enhanced release of ACTH. This claim is further supported by the fact that there were actually no ACTH increases measured at any time points studied immediately after STZ injection and neither during the first day after diabetes onset nor at later time points when diabetes is fully established (*i.e.* after 11 d of diabetes). At all time points, ACTH concentrations remained below control levels.

The enhanced adrenal sensitivity to ACTH becomes apparent already from the increased adrenal weight and is demonstrated *in vitro* in cultures derived from adrenal cells taken from diabetic mice. Cultures of the adrenal gland cells from diabetic mice challenged with ACTH result in B hypersecretion. We then hypothesized that besides adrenocortical growth, stimulation of adrenal MC2R and MC5R might be a possible mechanism by which low concentrations of ACTH could maintain B hypersecretion. Indeed, we found that ACTH receptors in the adrenals were up-regulated at 2 and 11 d of diabetes. The finding supports the hypothesis that a rapidly enhanced adrenal sensitivity to ACTH facilitates adaptation to the metabolic state induced by STZ in this diabetic model.

Other mechanisms inducing a rapid change in adrenal sensitivity could also be implicated. These mechanisms include splanchnic nerve input because splanchnic nerve stimulation was found to enhance the secretion of glucocorticoids in response to ACTH (24–28). Sympathetic innervation and thus catecholamines from the medulla may also participate as an ACTH-independent input to adrenocortical function (29–31). Adrenals also show a gated sensitivity to ACTH that is maintained in the absence of external signals but depends on the presence of a functional adrenal clockwork, which exerts its control on corticosteroid production and explains the circadian changes in adrenal sensitivity. In view of these findings, it has been suggested that light may directly entrain the adrenal clock via an autonomic input, thereby influencing circadian and possibly ultradian rhythms in B secretion (32, 33).

Other factors may be involved as well. 1) AVP exerts a

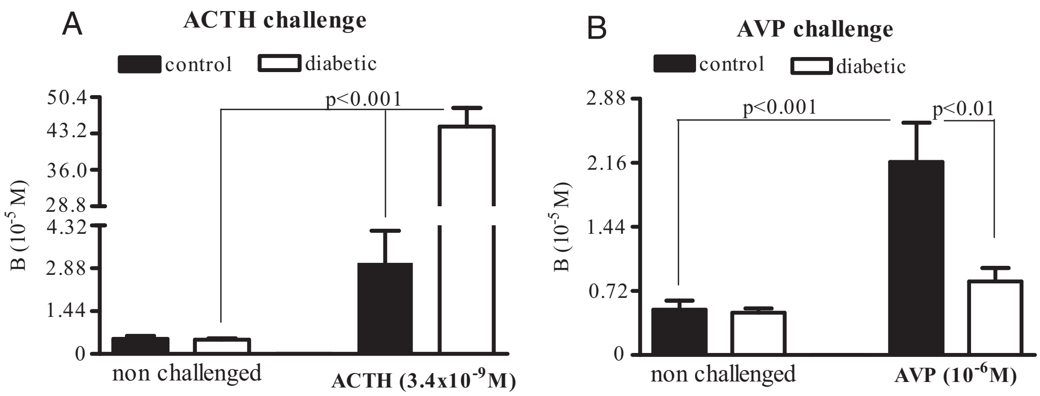


FIG. 3. Corticosterone secretion from adrenal cell cultures (10,000 cells/ml) after 60 min incubation with $3.4 \times 10^{-9}$ M of $ACTH_{1-24}$ (A) or $10^{-6}$ M of $AVP_{1-8}$ (B) from 11-d diabetic mice. *Black bars* represent cultured cells from control animals and *white bars* from chronic diabetic ones. Values are expressed mean ± SEM; n = 6–7. Nonchallenged indicates cultures from control and diabetic mice in which no ACTH or AVP were added.

direct stimulatory action on adrenocortical cells mediated through activation of typical V1aR. Our data demonstrate, however, that AVP does not mediate the hypercorticism in diabetes, because neither the B secretion from adrenocortical cultures nor adrenal V1aR expression was modulated compared with controls. 2) CRH/ACTH intraadrenal system can regulate adrenal steroidogenesis (29); a direct effect of CRH on adrenocortical steroidogenesis seems unlikely, because CRH had no effect on either isolated, dispersed adrenocortical cells (34) or on adrenocortical autotransplants deprived of chromaffin tissue.

An altered hippocampal input to the HPA axis was previously described in the STZ animal model of T1D (15, 35–38). However, discrepancies and similarities have been found in different models of T1D. Discrepancies are related to the HPA axis regulation. Chan *et al.* (15) reported a profound activation of the HPA axis in the rat model of STZ-induced diabetes, which was characterized by a marked increase in ACTH and B levels at 8 d after STZ injection. They found that the expression of AVP and CRH mRNAs in the hypothalamus and MR mRNA in the hippocampus was enhanced. Therefore, the authors suggested an increase in the central drive to the HPA axis that overrides the inhibitory influence of negative B feedback. Central to this reasoning was the up-regulation of MR in hippocampus, which is thought to modulate the inhibitory tone on HPA axis activity (39, 40).

In the present study, we found significant MR mRNA up-regulation in the CA1 area of the hippocampus only on the day of diabetes onset. However, at 11 d of diabetes, MR mRNA was significantly down-regulated in the hippocampus, which suggests that the inhibitory regulation on the HPA axis might be disrupted. This disruption could impair the shut-off response contributing to the observed chronic hypercorticism and could imply a time-dependent adaptation to the new metabolic condition. The nuclear MR in hippocampal neurons has a very high affinity to B and aldosterone, suggesting that this receptor is always extensively occupied. The MR signal is changed by altered receptor activity rather than ligand concentration. Hence, changes in nerve input have a profound influence on MR capacity (41). There is also a recently discovered membrane variant of the MR in the hippocampus, which may contribute to HPA axis regulation (42). Despite all these facts, we cannot offer an explanation why our results differ from those obtained by Chan *et al.* (15, 16).

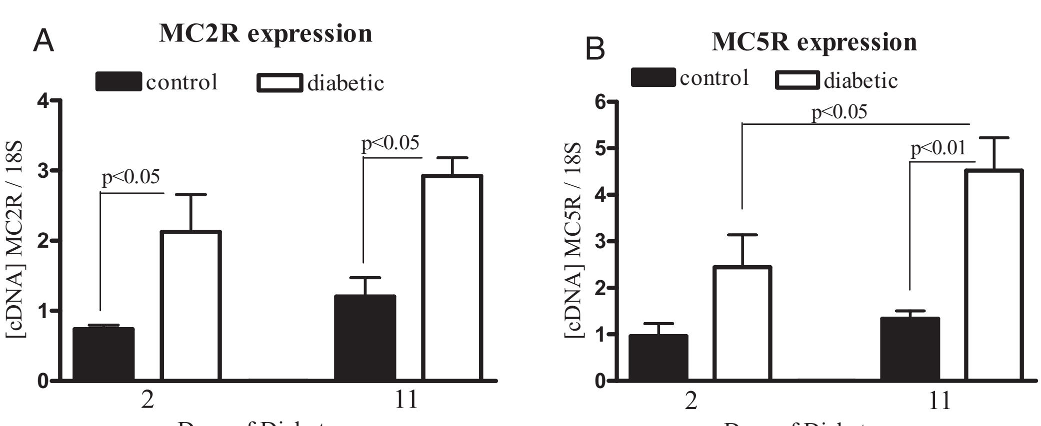


FIG. 4. ACTH (MC2 and MC5) receptor mRNA expression in the adrenal glands. Adrenal MC2R and MC5R mRNAs were measured with RT-qPCR, in control (*black bars*) and diabetic (*white bars*) animals at 2 and 11 d after STZ or vehicle injection. *Columns* represent mean ± SEM; n = 5.

**TABLE 2.** Hippocampal MR and GR and hypothalamic AVP, GR, and CRH mRNA expression at 2 and 11 d after diabetes onset

| | Hippocampus | | | PVN | | |
|---|---|---|---|---|---|---|
| | MR mRNA in DG | GR mRNA | | AVP mRNA | GR mRNA | CRH mRNA |
| | | CA1 | DG | | | |
| 2 d after diabetes onset | | | | | | |
| Control | 40.65 ± 10.82 | 41.58 ± 4.33 | 34.32 ± 1 | 50.79 ± 3.63 | 54.68 ± 13 | 109.7 ± 10 |
| Diabetic | 35.84 ± 4.20 | 42.66 ± 6.35 | 31.70 ± 4.34 | 66.73 ± 3.31[a] | 78.19 ± 6.54 | 88.33 ± 4 |
| 11 d after diabetes onset | | | | | | |
| Control | 69.69 ± 3.57 | 66.34 ± 4.42 | 63.49 ± 4 | 98.9 ± 10.21 | 76.19 ± 4.96 | 48.83 ± 3.74 |
| Diabetic | 58.88 ± 3.32[a] | 54.01 ± 3.91 | 58.94 ± 3.21 | 131.1 ± 3.79[b] | 65.01 ± 4.23 | 51.02 ± 3.95 |

mRNA expression is shown as OD (arbitrary units). Values are expressed as mean ± SEM; n = 7–8. The AVP mRNA quantification does not distinguish magnocellular from parvocellular cells. DG, Dentate gyrus.
[a] $P < 0.05$ *vs.* control.
[b] $P < 0.01$ *vs.* control.

Additional studies by Chan *et al.* (16) showed that adrenal sensitivity is not increased in uncontrolled STZ-diabetic animals as described before (37). They did not find a significant rise in B levels compared with controls after a low-dose ACTH stimulation test. Our data resemble, however, a study by Dallman *et al.* (43) showing that in response to food deprivation, elevated B levels occurred independent of an ACTH surge, suggesting an acute rise in adrenal sensitivity as the most proximal event. Another aspect of the study that remains unresolved is the question of how the thymus rapidly involutes in the face of moderately increased B levels in the STZ-treated animals.

Similarities in different models of the disease are also described in the literature: 1) decreased body weight gain and plasma insulin levels and increased food intake, water intake, plasma glucose, and B concentrations were reported in STZ-diabetic mice (8, 9 44) and rats (1, 7, 45), spontaneous T1D models such as the nonobese diabetic (NOD) mice (8, 46) and biobreeding rats (47, 48) and humans (49); 2) hippocampal alterations involving astrogliosis and decreased cell proliferation in STZ and NOD mice (8, 9, 44, 46) and STZ rats (50, 51); and 3) cognitive impairments in STZ-mice (Revsin, Y., N. V. Rekers, M. C. Louwe, F. E. Saravia, A. F. De Nicola, E. R. de Kloet, and M. S. Oitzl , submitted for publication), STZ rats (52), biobreeding rats (47), and humans (49). These similarities suggest no species differences and allow a generalization of the data we found in the STZ-diabetic mouse model.

The discrepancies between the present study and that of Chan *et al.* (15) could be explained by differences in the animal model used. First, although STZ-diabetic rats can survive up to 8 months (53), STZ-diabetic mice die a few months after onset of the disease (54, 55). Therefore, disparities in the severity of diabetes and routes of STZ administration and dosages (due to species variation in response to the drug) can contribute to the observed differences. In this regard, whereas a single STZ injection of 65 mg/kg body weight ip induces diabetes in rats, it does not induce the disease in mice, showing that mice are more resistant to the action of STZ on the destruction of the pancreatic $\beta$-cells. In our hands, we found that 170 mg/kg body weight ip is the minimum dose that induces diabetes in the c57BL/6 mice with the same diabetic parameters described in the literature indicative of T1D (blood glucose, insulin levels, and weight gain) (56, 57). Second, in the studies by Chan *et al.* (15, 16), animals treated with STZ were given 10% sucrose in drinking water for the first 24 h after the STZ injection to prevent hypoglycemia. It is noteworthy that this STZ model of T1D features moderate diabetes with hyperglycemia and moderately reduced fasting insulin levels. In our model, no sucrose was administered and hypoglycemia was observed 24 h after the STZ injection. Then from 48 h after STZ injection, the animals become hyperglycemic (Fig. 1A) with low insulin levels at fasting (1700 and 2000 h) and nonfasting (0900 and 1300 h) (Fig. 2C).

Besides the temporal changes in glucose and insulin levels close to STZ injection, B concentration increases 4 h after STZ injection and later on from 72 h, which corresponds to 24 h after the onset of hyperglycemia (Figs. 1A and 2B). It is known that this drug has toxic effects in the first hours after its administration (58); hence, the B hypersecretion 4 h after STZ administration might be due to the STZ cytotoxicity *per se*. The increased B concentration, before $\beta$-cell destruction (insulin increased at 8 h after STZ injection), followed by its decrease to control levels supports our assumption. Therefore, the later B hypersecretion 3 d after STZ injection might be the result of the rise in blood glucose levels (or its consequences). However, one cannot discard the possibility that the transient hypoglycemia 24 h after STZ injection may also be relevant for the later hypercorticism. Future studies in our model on sucrose administration after STZ injection (15, 16) or insulin replacement (59) will help to fully understand the observed differences between these two STZ models.

In the present study, we showed HPA axis modulation in STZ-diabetic mice at 2 and 11 d after diabetes onset. Moreover, we provided evidence that the up-regulation of adrenocortical ACTH receptors is an underlying mechanism responsible for the chronic hypercorticism in T1D. A better understanding of these mechanisms may open up new avenues for therapeutically useful strategies to normalize neuronal disturbances and improve cognitive disabilities of diabetic patients. Furthermore, the profound disturbance in the HPA axis regulation provides evidence for a role of B in diabetic neuropathology. Whether T1D leads to a more fragile state of the brain in which B excess may enhance the potential for damage and attenuate protective mechanisms, thus facilitating cognitive dysfunction and impair the ability to respond to stress, remains to be demonstrated.

In summary, in our mouse STZ model of T1D, the HPA axis readily reached a new setpoint characterized by high circulating B, low ACTH levels, and enhanced adrenocortical sensitivity. Surprisingly, ACTH levels were never elevated, also not at the onset of diabetes when hyperglycemia and later hypercorticism have developed. The up-regulation of ACTH receptors in the adrenal glands of STZ-induced diabetic mice might explain, at least in part, how hypercorticism is triggered and maintained. Moreover, the enhanced AVP mRNA in the PVN (also reported in the spontaneous T1D model, the NOD mouse) (60) and decreased MR mRNA in the dentate gyrus also may be considered manifestations of a profound disturbance in HPA axis regulation.

## Acknowledgments

We thank Dr. M. Frolich for the insulin measurement.

Received September 28, 2007. Accepted April 8, 2008.

Address all correspondence and requests for reprints to: Yanina Revsin, Division of Medical Pharmacology, LACDR. Einsteinweg 55, 2333CC, Leiden, The Netherlands. E-mail: y.revsin@lacdr.leidenuniv.nl.

This work was supported by grants from The Netherlands Organization for Scientific Research (NWO-WOTRO) Grant 88-252 and the Royal Netherlands Academy for Arts and Sciences.

Disclosure Statement: The authors of this manuscript have nothing to declare.

## References

1. **Magarinos AM, McEwen BS** 2000 Experimental diabetes in rats causes hippocampal dendritic and synaptic reorganization and increased glucocorticoid reactivity to stress. Proc Natl Acad Sci USA 97:11056–11061
2. **Gispen WH, Biessels GJ** 2000 Cognition and synaptic plasticity in diabetes mellitus. Trends Neurosci 23:542–549
3. **McCall AL** 2002 Diabetes mellitus and the central nervous system. Int Rev Neurobiol 51:415–453
4. **Artola A, Kamal A, Ramakers GM, Gardoni F, Di Luca M, Biessels GJ, Cattabeni F, Gispen WH** 2002 Synaptic plasticity in the diabetic brain: advanced aging? Prog Brain Res 138:305–314
5. **Biessels GJ, van der Heide LP, Kamal A, Bleys RL, Gispen WH** 2002 Ageing and diabetes: implications for brain function. Eur J Pharmacol 441:1–14
6. **Biessels GJ, Gispen WH** 2005 The impact of diabetes on cognition: what can be learned from rodent models? Neurobiol Aging 26(Suppl 1):36–41
7. **Kamal A, Biessels GJ, Gispen WH, Ramakers GM** 2006 Synaptic transmission changes in the pyramidal cells of the hippocampus in streptozotocin-induced diabetes mellitus in rats. Brain Res 1073–1074:276–280
8. **Saravia FE, Revsin Y, Gonzalez Deniselle MC, Gonzalez SL, Roig P, Lima A, Homo-Delarche F, De Nicola AF** 2002 Increased astrocyte reactivity in the hippocampus of murine models of type 1 diabetes: the nonobese diabetic (NOD) and streptozotocin-treated mice. Brain Res 957:345–353
9. **Revsin Y, Saravia F, Roig P, Lima A, de Kloet ER, Homo-Delarche F, De Nicola AF** 2005 Neuronal and astroglial alterations in the hippocampus of a mouse model for type 1 diabetes. Brain Res 1038:22–31
10. **Eichenbaum H** 2001 The hippocampus and declarative memory: cognitive mechanisms and neural codes. Behav Brain Res 127:199–207
11. **Eichenbaum H** 2004 Hippocampus: cognitive processes and neural representations that underlie declarative memory. Neuron 44:109–120
12. **Herman JP, Ostrander MM, Mueller NK, Figueiredo H** 2005 Limbic system mechanisms of stress regulation: hypothalamo-pituitary-adrenocortical axis. Prog Neuropsychopharmacol Biol Psychiatry 29:1201–1213
13. **Han F, Ozawa H, Matsuda KI, Lu H, de Kloet ER, Kawata M** 2007 Changes in the expression of corticotrophin-releasing hormone, mineralocorticoid receptor and glucocorticoid receptor mRNAs in the hypothalamic paraventricular nucleus induced by fornix transection and adrenalectomy. J Neuroendocrinol 19:229–238
14. **de Kloet ER, Joels M, Holsboer F** 2005 Stress and the brain: from adaptation to disease. Nat Rev Neurosci 6:463–475
15. **Chan O, Chan S, Inouye K, Vranic M, Matthews SG** 2001 Molecular regulation of the hypothalamo-pituitary-adrenal axis in streptozotocin-induced diabetes: effects of insulin treatment. Endocrinology 142:4872–4879
16. **Chan O, Inouye K, Vranic M, Matthews SG** 2002 Hyperactivation of the hypothalamo-pituitary-adrenocortical axis in streptozotocin-diabetes is associated with reduced stress responsiveness and decreased pituitary and adrenal sensitivity. Endocrinology 143:1761–1768
17. **Paxinos G, Frankling KB** 2001 The mouse brain in stereotaxic coordinates. 2nd ed. San Diego: Academic Press
18. **Cole TJ, Blendy JA, Schmid W, Strähle U, Schütz G** 1993 Expression of the mouse glucocorticoid receptor and its role during development. J Steroid Biochem Mol Biol 47:49–53
19. **Hesen W, Karst H, Meijer O, Cole TJ, Schmid W, de Kloet ER, Schütz G, Joëls M** 1996 Hippocampal cell responses in mice with a targeted glucocorticoid receptor gene disruption. J Neurosci 16:6766–6774
20. **Jingami H, Mizuno N, Takahashi H, Shibahara S, Furutani Y, Imura H, Numa S** 1985 Cloning and sequence analysis of cDNA for rat corticotropin-releasing factor precursor FEBS Lett 191:63–66
21. **Ludwig G, Hänze J, Lehmann E, Lang RE, Burbach JH, Ganten D** 1988 Measurement of mRNA by solution hybridization with $^{32}$P-labelled single stranded cRNA probe ("SP6 test"). Comparison with a $^{32}$P-labelled single stranded cDNA as hybridization probe ("S1 test") for measurement of AVP mRNA. Clin Exp Hypertens A 10:467–483
22. **Zhu LJ, Altmann SW** 2005 mRNA and 18S-RNA coapplication-reverse transcription for quantitative gene expression analysis. Anal Biochem 345:102–109
23. **Oitzl MS, van Haarst AD, Sutanto W, and de Kloet ER** 1995 Corticosterone, brain mineralocorticoid receptors (MRs) and the activity of the hypothalamic-pituitary-adrenal (HPA) axis: the Lewis rat as an example of increased central MR capacity and a hyporesponsive HPA axis. Psychoneuroendocrinology 20:655–675
24. **Edwards AV, Jones CT** 1987 The effect of splanchnic nerve stimulation on adrenocortical activity in conscious calves. J Physiol 382:385–396
25. **Bornstein SR, Ehrhart-Bornstein M, Scherbaum WA, Pfeiffer EF, Holst JJ** 1990 Effects of splanchnic nerve stimulation on the adrenal cortex may be mediated by chromaffin cells in a paracrine manner. Endocrinology 127:900–906
26. **Engeland WC** 1998 Functional innervation of the adrenal cortex by the splanchnic nerve. Horm Metab Res 30:311–314
27. **Ulrich-Lai YM, Engeland WC** 2002 Adrenal splanchnic innervation modulates adrenal cortical responses to dehydration stress in rats. Neuroendocrinology 76:79–92
28. **Ulrich-Lai YM, Arnhold MM, Engeland WC** 2006 Adrenal splanchnic innervation contributes to the diurnal rhythm of plasma corticosterone in rats by modulating adrenal sensitivity to ACTH. Am J Physiol Regul Integr Comp Physiol 290:R1128–R1135
29. **Ehrhart-Bornstein M, Hinson JP, Bornstein SR, Scherbaum WA, Vinson GP** 1998 Intraadrenal interactions in the regulation of adrenocortical steroidogenesis. Endocr Res 19:101–143
30. **Bornstein SR, Ehrhart-Bornstein M** 2000 Basic and clinical aspects of intraadrenal regulation of steroidogenesis. Z Rheumatol 59(Suppl 2):II/12–II/17
31. **Engeland WC, Arnhold MM** 2005 Neural circuitry in the regulation of adrenal corticosterone rhythmicity. Endocrine 28:325–332
32. **Jasper MS, Engeland WC** 1994 Splanchnic neural activity modulates ultradian and circadian rhythms in adrenocortical secretion in awake rats. Neuroendocrinology 59:97–109
33. **Oster H, Damerow S, Kiessling S, Jakubcakova V, Abraham D, Tian J, Hoffmann MW, Eichele G** 2006 The circadian rhythm of glucocorticoids is regulated by a gating mechanism residing in the adrenal cortical clock. Cell Metab 4:163–173
34. **van Oers JW, Hinson JP, Binnekade R, Tilders FJ** 1992 Physiological role of corticotropin-releasing factor in the control of adrenocorticotropin-mediated corticosterone release from the rat adrenal gland. Endocrinology 130:282–288
35. **De Nicola AF, Fridman O, Del Castillo EJ, Foglia VG** 1976 The influence of streptozotocin diabetes on adrenal function in male rats. Horm Metab Res 8:388–392
36. **Gibson MJ, De Nicola AF, Krieger DT** 1985 Streptozotocin-induced diabetes is associated with reduced immunoreactive $\beta$-endorphin concentrations in neurointermediate pituitary lobe and with disrupted circadian periodicity of plasma corticosterone levels. Neuroendocrinology 41:64–71
37. **Scribner KA, Walker CD, Cascio CS, Dallman MF** 1991 Chronic streptozotocin diabetes in rats facilitates the acute stress response without altering pituitary or adrenal responsiveness to secretagogues. Endocrinology 129:99–108
38. **Scribner KA, Akana SF, Walker CD, Dallman MF** 1993 Streptozotocin-diabetic rats exhibit facilitated adrenocorticotropin responses to acute stress, but normal sensitivity to feedback by corticosteroids. Endocrinology 133:2667–2674
39. **Ratka A, Sutanto W, Bloemers M, de Kloet ER** 1989 On the role of brain mineralocorticoid (type I) and glucocorticoid (type II) receptors in neuroendocrine regulation. Neuroendocrinology 50:117–123
40. **Reul JM, Gesing A, Droste S, Stec IS, Weber A, Bachmann C, Bilang-Bleuel A, Holsboer F, Linthorst AC** 2000 The brain mineralocorticoid receptor: greedy for ligand, mysterious in function. Eur J Pharmacol 405:235–249
41. **Kabbaj M, Morley-Fletcher S, Le Moal M, Maccari S** 2007 Individual differences in the effects of chronic prazosin hydrochloride treatment on hippocampal mineralocorticoid and glucocorticoid receptors. Eur J Neurosci 25:3312–3318
42. **Karst H, Berger S, Turiault M, Tronche F, Schutz G, Joels M** 2005 Mineralocorticoid receptors are indispensable for nongenomic modulation of hippocampal glutamate transmission by corticosterone. Proc Natl Acad Sci USA 102:19204–19207
43. **Dallman MF, Akana SF, Bhatnagar S, Bell ME, Choi S, Chu A, Horsley C,**

**Levin N, Meijer O, Soriano LR, Strack AM, Viau V** 1999 Starvation: early signals, sensors, and sequelae. Endocrinology 140:4015–40123
44. **Saravia F, Revsin Y, Lux-Lantos V, Beauquis J, Homo-Delarche F, De Nicola AF** 2004 Oestradiol restores cell proliferation in dentate gyrus and subventricular zone of streptozotocin-diabetic mice. J Neuroendocrinol 16:704–710
45. **Martinez-Tellez R, Gomez-Villalobos MJ, Flores G** 2005 Alteration in dendritic morphology of cortical neurons in rats with diabetes mellitus induced by streptozotocin. Brain Res 1048:108–115
46. **Beauquis J, Saravia F, Coulaud J, Roig P, Dardenne M, Homo-Delarche F, De Nicola A** 2007 Prominently decreased hippocampal neurogenesis in a spontaneous model of type 1 diabetes, the nonobese diabetic mouse. Exp Neurol 210:359–367
47. **Li ZG, Zhang W, Grunberger G, Sima AA** 2002 Hippocampal neuronal apoptosis in type 1 diabetes. Brain Res 946:221–231
48. **Li ZG, Zhang W, Sima AA** 2002 C-peptide prevents hippocampal apoptosis in type 1 diabetes. Int J Exp Diabetes Res 3:241–245
49. **Biessels GJ, Deary IJ, Ryan CM** 2008 Cognition and diabetes: a lifespan perspective. Lancet Neurol 7:184–190
50. **Baydas G, Reiter RJ, Yasar A, Tuzcu M, Akdemir I, Nedzvetskii VS** 2003 Melatonin reduces glial reactivity in the hippocampus, cortex, and cerebellum of streptozotocin-induced diabetic rats. Free Radic Biol Med 35:797–804
51. **Kang JO, Kim SK, Hong SE, Lee TH, Kim CJ** 2006 Low dose radiation overcomes diabetes-induced suppression of hippocampal neuronal cell proliferation in rats. J Korean Med Sci 21:500–505
52. **Zhou J, Wang L, Ling S, Zhang X** 2007 Expression changes of growth-associated protein-43 (GAP-43) and mitogen-activated protein kinase phosphatase-1 (MKP-1) and in hippocampus of streptozotocin-induced diabetic cognitive impairment rats. Exp Neurol 206:201–208
53. **Schmidt RE, Dorsey DA, Beaudet LN, Parvin CA, Zhang W, Sima AA** 2004 Experimental rat models of types 1 and 2 diabetes differ in sympathetic neuroaxonal dystrophy. J Neuropathol Exp Neurol 63:450–460
54. **Paik SG, Fleischer N, Shin SI** 1980 Insulin-dependent diabetes mellitus induced by subdiabetogenic doses of streptozotocin: obligatory role of cell-mediated autoimmune processes. Proc Natl Acad Sci USA 77:6129–6133
55. **Teta M, Long SY, Wartschow LM, Rankin MM, Kushner JA** 2005 Very slow turnover of $\beta$-cells in aged adult mice. Diabetes 54:2557–2567
56. **McNeill JH** 1999 Experimental models of diabetes. Boca Raton, FL: CRC Press
57. **Lin CY, Higginbotham DA, Judd RL, White BD** 2002 Central leptin increases insulin sensitivity in streptozotocin-induced diabetic rats. Am J Physiol Endocrinol Metab 282:E1084–E1091
58. **Bolzan AD, Bianchi MS** 2002 Genotoxicity of streptozotocin. Mutat Res 512:121–134
59. **Inouye KE, Yue JT, Chan O, Kim T, Akirav EM, Park E, Riddell MC, Burdett E, Matthews SG, Vranic M** 2006 Effects of insulin treatment without and with recurrent hypoglycemia on hypoglycemic counterregulation and adrenal catecholamine-synthesizing enzymes in diabetic rats. Endocrinology 147:1860–1870
60. **Saravia F, Gonzalez S, Roig P, Alves V, Homo-Delarche F, De Nicola AF** 2001 Diabetes increases the expression of hypothalamic neuropeptides in a spontaneous model of type I diabetes, the nonobese diabetic (NOD) mouse. Cell Mol Neurobiol 21:15–27

***Endocrinology* is published monthly by The Endocrine Society (http://www.endo-society.org), the foremost professional society serving the endocrine community.**